ELSEVIER

Microelectronics Journal 33 (2002) 733–738

Microelectronics Journal

www.elsevier.com/locate/mejo

Application of Green's functions for analysis of transient thermal states in electronic circuits

Marcin Janicki[a,*], Gilbert De Mey[b], Andrzej Napieralski[a]

[a]*Department of Microelectronics and Computer Science, Technical University of Lodz, Al. Politechniki 11, 93-590 Lodz, Poland*
[b]*Department of Electronics and Information Systems, University of Ghent, St. Pietersnieuwstraat 41, 9000 Ghent, Belgium*

Accepted 21 May 2002

Abstract

This paper presents an approach to the modelling of transient thermal states in electronic circuits using an analytical solution of the heat equation. Fully three-dimensional analytical time dependent solutions are determined with the help of Green's functions. The solution method is illustrated in detail on a practical example, where the results of transient thermal simulations of a real hybrid circuit are compared with infrared measurements.

Keywords: Transient thermal simulation; Electronic circuit; Infrared measurement

1. Introduction

Owing to recent technological advances, it was possible not only to miniaturise devices further, but also to increase their operating frequency. This, in turn, augmented significantly the dissipated power density. Since cooling problems occur now even in typically low power applications, still more and more products must undergo in their design process a rigorous thermal simulation. Therefore, the need has arisen for reliable circuit thermal models and simulation tools capable of performing a fast but accurate thermal analysis of a particular prototype.

Most currently available thermal simulators are based on numerical methods for the solution of the heat equation such as the finite difference method or the boundary element method. Unfortunately, in order to obtain accurate results applying numerical methods, it is necessary to use a dense structure meshing, especially where the temperature gradient is important requiring a lot of computation time. Nowadays, the generally accepted procedure to create a thermal model is as follows. First, the full thermal model of a system is simulated applying different boundary conditions. Then, assuming some error minimisation criteria, the model is reduced resulting in a fairly boundary independent one, which could in turn be included in some electro-thermal simulator.

Regarding costs and time of a design process, the analytical solutions giving explicit formulas relating power dissipation to temperature rise at any point in a structure would be much more desirable, but usually they are difficult to find. However, as will be shown in this paper, there exists large group of circuits, which can be modelled with satisfactory accuracy by simple thermal models. For such models, it is possible to find analytical solutions of the heat equation.

The contents of the paper can be divided into two parts: a theoretical and an experimental one. The first part consists of two sections, which cover briefly the theoretical background concerning the heat equation and the Green's functions (GFs), respectively. Then, in the experimental part, the theory is applied for transient thermal simulation of the heating and the cooling processes of a hybrid circuit. The simulation results are compared with infrared thermal measurements providing some important conclusions and indications for future work.

2. Heat equation

From the theory of heat transfer, it is known that in most cases the heat conduction process obeys the Fourier law, which states that the heat flux is proportional to the temperature gradient. When the thermal conductivity is constant, the energy balance for an arbitrary volume leads to

* Corresponding author. Tel.: +48-42-631-2645; fax: +48-42-636-0327.
E-mail address: janicki@dmcs.p.lodz.pl (M. Janicki).

0026-2692/02/$ - see front matter
PII: S0026-2692(02)00057-5

the following three-dimensional heat equation

$$\nabla^2 T + \frac{g_v}{\lambda} = \frac{1}{\alpha}\frac{\partial T}{\partial t} \tag{1}$$

where α is the thermal diffusivity (m^2/s); T, the temperature (K); λ, the thermal conductivity (W/m K); g_v, the generated heat per unit volume (W/m^3); t is the time (s).

Furthermore, for homogenous isotropic solids without internal heat generation, which is the case considered in this paper, Eq. (1) takes the form of the diffusion equation:

$$\alpha\nabla^2 T = \frac{\partial T}{\partial t} \tag{2}$$

In order to solve the above equation, the thermal diffusivity as well as the initial and boundary conditions must be determined. There are three basic kinds of boundary conditions describing the heat exchange at the structure boundaries: Dirichlet condition (prescribed temperature), Neumann condition (prescribed heat flux) or Robin condition (convective condition). Heat generated in electronic circuits is conducted towards the structure edges where it is removed by means of convection or radiation. Thus, based on Fourier's and Newton's law, the heat removal at structure surface can be represented optimally by the third kind of boundary condition expressed by the following equation

$$q = -\lambda\frac{\partial T}{\partial n} = h(T - T_\infty) \tag{3}$$

where q is the heat flux (W/m^2); n, the normal to surface; h, the heat exchange coefficient (W/m^2 K); T, the surface temperature (K); T_∞ is the surrounding fluid temperature (K).

The methods for solving the heat equation can be divided into two general groups: analytical and numerical ones. In this publication, the authors focused on the particular analytical method employing GFs, which is described in Section 3. Generally, analytical methods allow solutions in the form of a single formula for the whole structure. However, in most cases it is difficult to find such a solution because of the fact that real structures have very complex shapes or boundary conditions.

Fortunately, many electronic circuits have relatively simple shapes and analytical methods can be successfully applied for their analysis. Then, if a thermal model is not excessively simplified, analytical solutions are more accurate than numerical ones, which inherently are not exact and depend on the choice of structure discretisation mesh. More information on the heat equation and the different solution methods, both numerical and analytical, can be found in Refs. [1–4].

3. Green's functions and their interpretation

GFs are powerful mathematical tools suitable for obtaining solutions of linear heat conduction problems. There are two possible interpretations of GFs. Firstly, they can be regarded as a temperature response at a point r at time t caused by an instantaneous energy generation at a point r' at time τ. Thus, theoretically, in order to obtain the temperature response in time, it is sufficient to integrate the GF over all points and times at which energy is generated. Alternatively, a GF is the temperature response at a point r in time t due to the initial temperature rise at a point r'. Then, the temperature distribution is obtained as an integral of a GF evaluated at time 0 over the whole analysis domain.

Particular forms of GFs depend only on the structure geometry and the applied boundary conditions. Therefore, the same GF can be used then for solving all the problems, whatever temperature distribution results from. Namely, for linear problems the overall temperature rise can be computed as the sum of the individual temperature rises caused by all the contributing factors, such as the initial temperature distribution, the internal energy generation or the non-homogeneous boundary conditions, as shown for the one-dimensional case in Eq. (4). For the full derivation of the equation, refer to Beck et al. [4].

$$\text{Initial distribution}: \qquad T(x,t) = \int_{x'=0}^{L} G(x,t|x',0)\,\mathrm{d}x' \tag{4a}$$

energy generation :

$$+\int_{\tau=0}^{t}\int_{x'=0}^{L}\frac{\alpha}{\lambda}G(x,t|x',\tau)g(x',\tau)\,\mathrm{d}x'\,\mathrm{d}\tau \tag{4b}$$

$$\text{prescribed temperature}: \qquad -\int_{\tau=0}^{t}\alpha T(\tau)\left.\frac{\partial G}{\partial n'}\right|_{x'=x_i}\mathrm{d}\tau \tag{4c}$$

$$\text{prescribed heat flux}: \qquad +\int_{\tau=0}^{t}\frac{\alpha}{\lambda}q(\tau)G(x,t|x_i,\tau)\,\mathrm{d}\tau \tag{4d}$$

$$\text{convective condition}: \qquad +\int_{\tau=0}^{t}\frac{\alpha}{\lambda}hT_\infty G(x,t|x_i,\tau)\,\mathrm{d}\tau \tag{4e}$$

where L is the structure length (m) and i is the non-homogeneous boundary index.

The GF in the first component on the right-hand side of the above equation should be evaluated for the time τ equal to 0. The last three terms are given here for the sake of formula integrity but they have to be computed only when a given boundary condition is non-homogeneous. Then, the value of the GF, or its derivative, is evaluated for x' equal to the co-ordinate of the particular boundary, i.e. 0 or L in the one-dimensional case.

Since GFs are basic, geometry dependent, solutions of specific differential equations with homogenous boundary conditions, they can be easily tabulated and used for construction of other more complex solutions. For example, as it will be demonstrated later, in many cases, especially in the rectangular co-ordinate system,

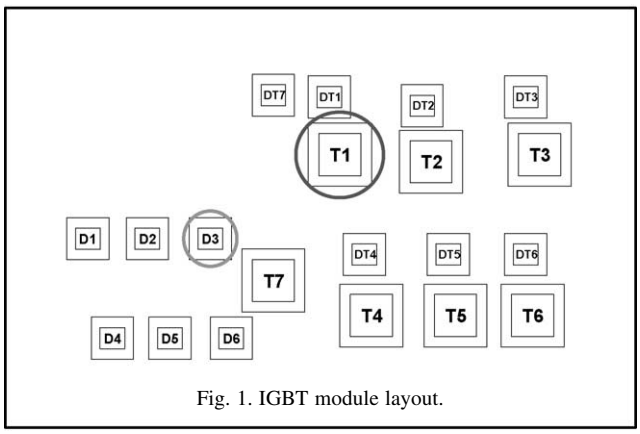

Fig. 1. IGBT module layout.

two- or three-dimensional GFs can be found by a simple multiplication of the one-dimensional GFs.

The GFs can be derived using different methods, such as the method of images, the Laplace transform method or the Fourier method of separation of variables. All these methods lead to solutions in different forms of mathematically equivalent expressions. From the computational point of view, the main difference between the methods is the series convergence, which in turn determines the simulation time. Usually, the first two methods yield series, which are rapidly convergent for low Fourier numbers up to 0.05–0.2 and the Fourier method produces series, which are better convergent for large Fourier numbers. The dimensionless Fourier number Fo can be found from the following formula:

$$Fo = \frac{\alpha t}{l^2} \tag{5}$$

The symbol l in the denominator denotes any distance for which the speed of the heat diffusion is assessed, in particular it could be the dimension of a structure. For the materials commonly encountered in electronics, the limit value of the Fourier number corresponds to the time in the range from several milliseconds up to a few seconds, which is substantially smaller than both heating and cooling processes for the circuit under consideration. Therefore, the authors focused in this paper only on the so-called large time GFs obtained using the Fourier method. Nevertheless, all the presented considerations remain valid, though for shorter times it might be advisable to use the small time GFs. More information on GFs and methods of driving them can be found in Refs. [4–7].

4. Hybrid circuit and its thermal model

The circuit analysed in this paper is a prototype three-phase AC motor driver realised as an IGBT power module

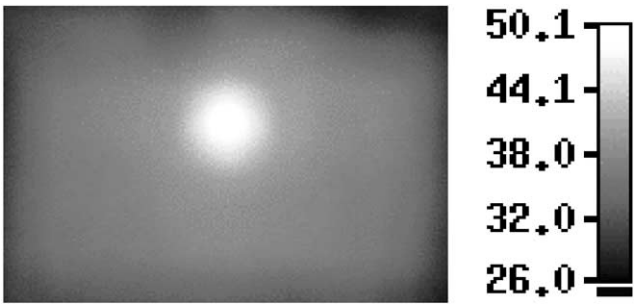

Fig. 2. Infrared image for cooling process after 120 s.

manufactured in the Insulated Metal Substrate hybrid technology. The circuit, shown in Fig. 1, consists of the IGBT transistors T1–T7, the rectifying diodes D1–D6 and the protection diodes DT1–DT7. All the silicon devices together with the molybdenum heat spreaders are mounted on a large 50 mm × 75 mm × 1.5 mm aluminium plate insulated by a thin raising layer. More about the circuit itself can be found in Ref. [8].

The circuit cooling and heating processes were investigated for the particular case when a power of 8.4 W was dissipated in transistor T1. During the measurements, the circuit was placed horizontally between thermally insulated clamps and cooled by means of radiation and natural convection. The circuit transient temperature measurements were taken using the AGEMA Thermovision 900 infrared camera. An example of an infrared image is shown in Fig. 2. Before the measurements, in order to assure uniform emissivity, the surface of the circuit was sprayed with black matt paint. During the measurements, the ambient temperature was equal to 21.5 °C. The complete heating and cooling curves obtained for the hot spot (transistor T1) and the diode D3 are presented together with the simulation results in Figs. 4 and 5.

Before the actual simulations a simple but accurate thermal model of the circuit had to be created. The model should allow the application of the presented earlier analytical solution method yet providing satisfactory accuracy. Initially, a full five-layer three-dimensional thermal model of the circuit was created based on the geometrical and material data provided by the manufacturer. Then, the temperature distribution in the structure was computed using the numerical finite difference method. The simulations showed that the temperature drop in the upper layers of the circuit was not significant, thus the original thermal model was considerably reduced by omitting all the layers except the substrate aluminium plate. Owing to the model reduction, it was possible to use the analytical GF method for transient thermal simulations. The final one-layer circuit thermal model is presented in Fig. 3. More detailed considerations in the model itself and the process of its creation can be found in Ref. [9].

As can be seen, the heat generated in the IGBT

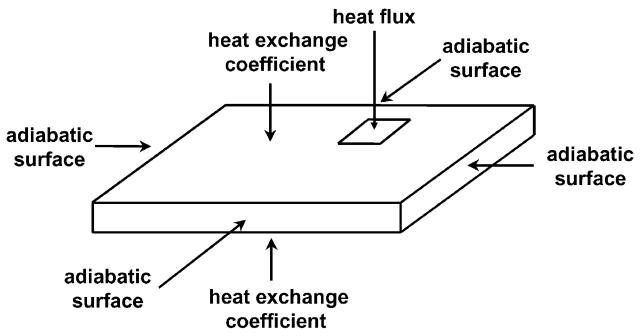

Fig. 3. Circuit thermal model.

transistor is represented in the model by the heat flux penetrating into the structure through its top surface. Because the circuit is relatively thin in comparison to its area, it is assumed that the heat flows vertically. Hence the four lateral surfaces of the aluminium plate are regarded as adiabatic and the heat is removed only at the two remaining surfaces, which is modelled by the heat transfer coefficient. The model is summarised in the following equations:

$$\text{Heat equation :} \qquad \lambda\nabla^2 T = \rho c\frac{\partial T}{\partial t} \tag{6}$$

Boundary conditions:

$$\text{Top surface :} \qquad -\lambda\frac{\partial T}{\partial n} = h(T - T_\infty) \tag{7a}$$

$$\text{Lateral surfaces :} \qquad \frac{\partial T}{\partial n} = 0 \tag{7b}$$

$$\text{Bottom surface :} \qquad -\lambda\frac{\partial T}{\partial n} = h(T - T_\infty) \tag{7c}$$

5. Heat equation solution and circuit simulations

Given the thermal model of the circuit, the solution of the heat equation was determined in accordance with the outline of the method suggested by Beck et al. in Ref. [5]. The first step was to determine the three one-dimensional GFs for each of the co-ordinates. These functions were found employing by the Fourier separation of variables method for the specific boundary conditions consistent with Eq. (7). The resulting one-dimensional GFs are as follows

$$G_x(x,t|x',\tau) = \frac{1}{a}\left[1 + 2\sum_{m=1}^{\infty}\exp\left(-\left(\frac{m\pi}{a}\right)^2\alpha(t-\tau)\right)\right.$$
$$\left.\times\cos\left(\frac{m\pi}{a}x\right)\cos\left(\frac{m\pi}{a}x'\right)\right] \tag{8a}$$

$$G_y(y,t|y',\tau) = \frac{1}{b}\left[1 + 2\sum_{n=1}^{\infty}\exp\left(-\left(\frac{n\pi}{b}\right)^2\alpha(t-\tau)\right)\right.$$
$$\left.\times\cos\left(\frac{n\pi}{b}y\right)\cos\left(\frac{n\pi}{b}y'\right)\right] \tag{8b}$$

$$G_z(z,t|z',\tau) = \frac{2}{d}\sum_{k=1}^{\infty}\frac{\exp\left(-\left(\frac{\beta_k}{d}\right)^2\alpha(t-\tau)\right)}{\beta_k^2 + \left(\frac{hd}{\lambda}\right)^2 + \frac{2hd}{\lambda}}$$
$$\times\left(\beta_k\cos\left(\frac{\beta_k}{d}z\right) + \frac{hd}{\lambda}\sin\left(\frac{\beta_k}{d}z\right)\right)$$
$$\times\left(\beta_k\cos\left(\frac{\beta_k}{d}z'\right) + \frac{hd}{\lambda}\sin\left(\frac{\beta_k}{d}z'\right)\right) \tag{8c}$$

where G is the Green's function; x, y, z, x', y' and z', the co-ordinates (m); t, τ, the time (s); a, b and d, the circuit dimensions in x, y and z direction, respectively (m); m, n and k, the series indices; β_k, the positive solutions of the equation: $\tan\beta_k = 2\beta_k hd/\lambda(\beta_k^2 - (hd/\lambda)^2)$.

Next, the one-dimensional GFs G_x, G_y, and G_z from Eq. (8) were multiplied in order to obtain the three-dimensional GF valid for the whole structure. When investigating the heating process, the temperature rise in the circuit is not influenced by the initial temperature distribution and there is no internal energy generation. Since the only one non-homogenous boundary condition in this case is the heat flux diffusing into the structure through its top surface, the temperature rise can be calculated performing an integration over time and space as shown in Eq. (9). Comparing to the one-dimensional Eq. (4), additional integration over the entire non-homogeneous boundary was introduced. Accordingly, all the integrals over x' should be transformed in the three-dimensional case into volume integrals

$$T(x,y,z,t) = \frac{\alpha q}{\lambda}\int_{\tau=0}^{t}\int_{y'=y1}^{y2}\int_{x'=x1}^{x2} G_x(x,t|x',\tau)$$
$$\times G_y(y,t|y',\tau)G_z(z,t|0,\tau)\,\mathrm{d}x'\,\mathrm{d}y'\,\mathrm{d}\tau \tag{9}$$

where $x1$, $x2$, $y1$ and $y2$ are the heat source boundary co-ordinates (m).

Then, based on Eqs. (8) and (9), it is possible to find the final solution as a sum of four series given in Eq. (10). The series are theoretically infinite, but in practice the series components are rapidly convergent to 0, thus the series can be truncated without any serious impact on the results. For example, in the simulations conducted with 5-digit

precision, it was enough to compute only the first 30 series components even for the shortest times.

$$T(x,y,z,t) = \frac{2qd(x2-x1)(y2-y1)}{ab\lambda}$$
$$\times\sum_{k=1}^{\infty}\frac{1-\exp\left(-\alpha t\left(\frac{\beta_k}{d}\right)^2\right)}{\beta_k\left(\beta_k^2+\frac{2hd}{\lambda}+\left(\frac{hd}{\lambda}\right)^2\right)}\left(\beta_k\cos\left(\frac{\beta_k}{d}z\right)+\frac{hd}{\lambda}\sin\left(\frac{\beta_k}{d}z\right)\right)+\frac{4q(y2-y1)}{\pi bd\lambda}\sum_{m=1}^{\infty}$$
$$\times\sum_{k=1}^{\infty}\frac{1-\exp\left(-\alpha t\left(\left(\frac{m\pi}{a}\right)^2+\left(\frac{\beta_k}{d}\right)^2\right)\right)}{\frac{m}{\beta_k}\left(\left(\frac{m\pi}{a}\right)^2+\left(\frac{\beta_k}{d}\right)^2\right)\left(\beta_k^2+\frac{2hd}{\lambda}+\left(\frac{hd}{\lambda}\right)^2\right)}$$
$$\times\left(\sin\left(\frac{m\pi}{a}x2\right)-\sin\left(\frac{m\pi}{a}x1\right)\right)\left(\beta_k\cos\left(\frac{\beta_k}{d}z\right)+\frac{hd}{\lambda}\sin\left(\frac{\beta_k}{d}z\right)\right)\cos\left(\frac{m\pi}{a}x\right)+\frac{4q(x2-x1)}{\pi a\,\mathrm{d}\lambda}\sum_{n=1}^{\infty}$$
$$\times\sum_{k=1}^{\infty}\frac{1-\exp\left(-\alpha t\left(\left(\frac{n\pi}{b}\right)^2+\left(\frac{\beta_k}{d}\right)^2\right)\right)}{\frac{n}{\beta_k}\left(\left(\frac{n\pi}{b}\right)^2+\left(\frac{\beta_k}{d}\right)^2\right)\left(\beta_k^2+\frac{2hd}{\lambda}+\left(\frac{hd}{\lambda}\right)^2\right)}$$
$$\times\left(\sin\left(\frac{n\pi}{b}y2\right)-\sin\left(\frac{n\pi}{b}y1\right)\right)\left(\beta_k\cos\left(\frac{\beta_k}{d}z\right)+\frac{hd}{\lambda}\sin\left(\frac{\beta_k}{d}z\right)\right)\cos\left(\frac{n\pi}{b}y\right)+\frac{8q}{\pi^2\,\mathrm{d}\lambda}\sum_{m=1}^{\infty}\sum_{n=1}^{\infty}\sum_{k=1}^{\infty}$$
$$\times\frac{1-\exp\left(-\alpha t\left(\left(\frac{m\pi}{a}\right)^2+\left(\frac{n\pi}{b}\right)^2+\left(\frac{\beta_k}{d}\right)^2\right)\right)}{\frac{mn}{\beta_k}\left(\left(\frac{m\pi}{a}\right)^2+\left(\frac{n\pi}{b}\right)^2+\left(\frac{\beta_k}{d}\right)^2\right)\left(\beta_k^2+\frac{2hd}{\lambda}+\left(\frac{hd}{\lambda}\right)^2\right)}$$
$$\times\left(\sin\left(\frac{m\pi}{a}x2\right)-\sin\left(\frac{m\pi}{a}x1\right)\right)\left(\sin\left(\frac{n\pi}{b}y2\right)-\sin\left(\frac{n\pi}{b}y1\right)\right)\left(\beta_k\cos\left(\frac{\beta_k}{d}z\right)+\frac{hd}{\lambda}\sin\left(\frac{\beta_k}{d}z\right)\right)$$
$$\times\cos\left(\frac{m\pi}{a}x\right)\cos\left(\frac{n\pi}{b}y\right) \qquad (10)$$

Because the whole circuit has been simulated as a single layer, it was necessary to perform preliminary simulations in order to determine in advance the equivalent values of the model parameters, such as the average heat transfer coefficient h, the thermal conductivity λ and the thermal diffusivity α. These values were set experimentally by minimising the relative error with respect to the measurements.

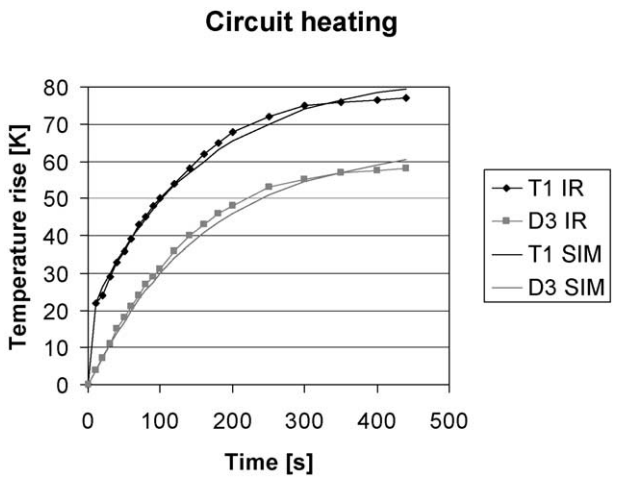

Fig. 4. Circuit heating-measurement and simulation.

The thermal conductivity influences mainly the temperature difference between selected locations and the heat exchange coefficient is responsible for the overall temperature rise value, so these two parameter values were determined from the steady-state asymptotic temperature values. Conversely, the thermal diffusivity value was found directly from the transient temperature curve so as to get the correct temperature rise rate. The resulting simulation results are compared with the measurements in Figs. 4 and 5.

As can be seen from the above charts, this simple thermal model proved to be quite accurate. The differences between simulated and measured temperature values do not exceed 3 K, which is comparable to the accuracy of the infrared measurement. The main discrepancy resides in the shape of the curve. Namely, the measured values seem not to obey the exponential dependence of temperature on time. This phenomenon can be explained by the fact that the real circuit consists of many various materials and the obtained curve is the superposition of a few separate curves. Moreover, the thermal model is linear which implies that

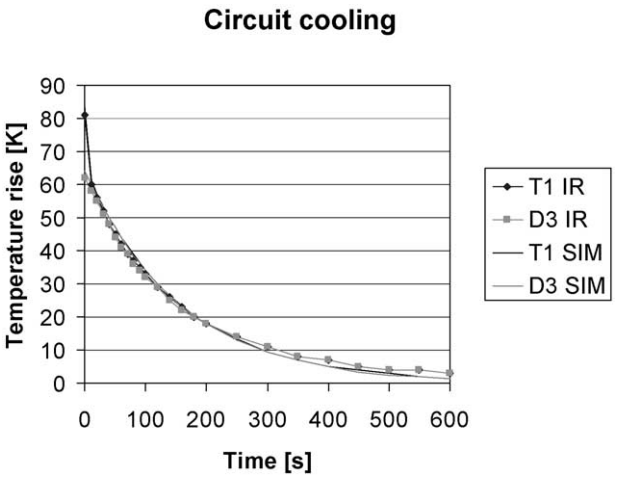

Fig. 5. Circuit cooling-measurement and simulation.

the thermal conductivity is temperature independent, which obviously is not true.

Another source of errors is the assumption on the uniformity of the heat exchange coefficient. The coefficient value is certainly much higher in the region close to the heat source due to the more important temperature difference between the circuit surface and the surrounding air.

Another issue that should be commented on is the equivalent values of the parameters resulting from the thermal model optimisation. The thermal conductivity value of 102 W/m K is approximately equal to half of the conductivity of aluminium and is comparable to the one of silicon, which proves that the base plate material is a relatively good thermal conductor. The average value of the heat exchange coefficient reflecting the joint radiation and convection cooling mechanisms is equal to 17.4 W/m^2 K, which is also acceptable in the considered temperature range. On the other hand, the diffusivity value of 2.1×10^{-5} m^2/s is an order of magnitude lower than the one for aluminium. This is probably due to the fact that the real thermal path is much longer than the one employed in the thermal model because the generated heat must first diffuse through the silicon structures and head spreaders, which is not taken into account in the model.

6. Conclusions

The results of the research presented in this paper are very promising. Although the proposed thermal model is extremely simple, the obtained simulation accuracy is quite satisfactory. The accuracy could be further improved developing the method by allowing the analysis of multilayer structures.

The demonstrated method is not limited only to the particular set of boundary conditions applied in the simulations. The solution of the heat equation could be easily adopted for other types of boundary conditions. As already mentioned, GFs depend only on a particular geometry and boundary conditions, thus the same GF can be used for evaluating the temperature rise caused by different factors. Moreover, for linear problems, the combined impact of different factors influencing the temperature rise can be found by a simple superposition of their effects.

Although in the considered case, it was possible to find analytically the final formula describing the temperature of the structure, in some more complex cases numerical evaluation of integrals might be required.

The density of the dissipated power (heat flux) is an explicit factor in the final analytical solution of the heat equation, which is particularly convenient for the applications where the temperature at selected locations is repeatedly computed for different values of the dissipated power. In this case, when using numerical methods, the whole set of difference equations would have to be solved again. This is not required in the case of an analytical method because the coefficients relating to the power dissipation to the temperature rise needs to be evaluated only once.

Thus, the presented method might prove to be competitive with numerical methods in the applications where the temperature has to be computed only at a limited number of locations, e.g. in the hot spots. However, because the computation time depends strongly on the number of locations and time instants at which temperature value is to be evaluated, numerical methods might be preferred if the whole temperature distribution map has to be found.

Acknowledgments

This work was supported by the NATO Advanced Fellowship Programme and the university internal grant K-25/Dz.St./1/02.

References

[1] Y. Bayazitoglu, M.N. Ozisik, Elements of Heat Transfer, McGraw-Hill, New York, 1988.
[2] M.N. Ozisik, Heat Conduction, Wiley, New York, 1993.
[3] J.P. Holman, Heat Transfer, McGraw-Hill, New York, 1985.
[4] H.S. Carslaw, J.S. Jaeger, Conduction of Heat in Solids, Clarendon Press, Oxford, 1947.
[5] J.V. Beck, K.D. Cole, A. Haji-Sheikh, B. Litkouhi, Heat Conduction Using Green's Functions, Hemisphere, Washington, DC, 1992.
[6] M.D. Greenberg, Application of Green's Functions in Science and Engineering, Prentice-Hall, Englewood Cliffs, NJ, 1971.
[7] I. Stakgold, Green's Functions and Boundary Value Problems, Willey-Interscience, New York, 1979.
[8] Janicki M, Kawka P, De Mey G, Napieralski A. IGBT hybrid module thermal measurements and simulations. Proceedings of the Eighth International Conference Mixdes 2001, Zakopane, Poland; 21–23 June 2001. p. 249–252.
[9] Janicki M, Napieralski A. IGBT module thermal simulation. Proceedings of the Ninth European Conference on Power Electronics and Applications EPE, Graz, Austria; 27–29 August 2001. DS2.2-2.